Iridium(III) Amine Complexes as High-Stability Structure-Directing Agents for the Synthesis of Metal Phosphates

D. J. Williams,[†] J. S. Kruger,[‡] A. F. McLeroy,[‡] A. P. Wilkinson,*[,‡] and J. C. Hanson[§]

Chemistry Department, Kennesaw State University, Marietta, Georgia 30061, School of Chemistry and Biochemistry, Georgia Institute of Technology, Atlanta, Georgia 30332-0400, and Chemistry Department, Brookhaven National Laboratory, Upton, Long Island, New York 11973

Received April 5, 1999. Revised Manuscript Received June 7, 1999

The metal complexes $Ir(en)_3^{3+}$ and $M((\pm)chxn)_3^{3+}$ (en = 1,2-diaminoethane, chxn = *trans*-1,2-diaminocyclohexane, M = Ir or Co) have been used to synthesize the layered compound Δ,Λ-$Ir(en)_3[Al_3P_4O_{16}]\cdot xH_2O$ ($x \approx 3.45$) and the chain compounds $M(chxn)_3[Al_2P_3O_{12}]\cdot xH_2O$ ($x \approx 4$). The chain compounds contain two of the eight possible isomeric forms of the cation, $\Lambda(lel_2ob)$-[M(*S,S*-chxn)$_2$(*R,R*-chxn)]$^{3+}$ and its mirror image $\Delta(lel_2ob)$-[M(*R,R*-chxn)$_2$(*S,S*-chxn)]$^{3+}$. Microcrystals of the $Ir(en)_3^{3+}$ and $Ir(chxn)_3^{3+}$ containing AlPOs were structurally characterized using synchrotron radiation. Δ,Λ-$Ir(en)_3[Al_3P_4O_{16}]\cdot xH_2O$ is isomorphous with the previously reported material Δ,Λ-$Co(en)_3[Al_3P_4O_{16}]\cdot xH_2O$. The materials prepared using $Co((\pm)chxn)_3^{3+}$ and $Ir((\pm)chxn)_3^{3+}$ are also isostructural with one another and contain a new type of aluminophosphate chain. The use of Ir(III) in the structure-directing metal complex enabled the use of much harsher hydrothermal conditions for the metal phosphate synthesis than could be employed with the corresponding Co(III) complexes. $Ir(C_2N_2H_8)_3[Al_3P_4O_{16}]\cdot 3.45H_2O$: $M_r = 895.5$, orthorhombic, *Pnna*, $a = 8.548(5)$, $b = 21.983(14)$, $c = 13.970(9)$ Å, $V = 2625(3)$ Å^3, $Z = 4$, $\rho_{calc} = 2.266$ g cm^{-3}, $\lambda = 1.1167$ Å, $\mu = 14.03$ mm^{-1}, $F(000) = 1762$, $T = 293$ K, $R_F = 0.128$ for 954 reflections $I > 2\sigma(I)$. $Ir(C_6N_2H_{14})_3Al_2P_3O_{12}\cdot 4H_2O$: $M_r = 945.7$, triclinic, $P\bar{1}$, $a = 9.649(5)$, $b = 12.365(9)$, $c = 16.083(8)$ Å, $\alpha = 100.02(6)$, $\beta = 101.64(5)$, $\gamma = 104.75(6)°$, $V = 1765(2)$ Å^3, $Z = 2$, $\rho_{calc} = 1.779$ g cm^{-3}, $\lambda = 1.1167$ Å, $\mu = 9.747$ mm^{-1}, $F(000) = 952$, $T = 293$ K, $R_F = 0.128$ for 966 reflections $I > 2\sigma(I)$.

Introduction

The synthesis of new aluminosilicate and aluminophosphate framework materials is closely linked to the chemist's ability to devise new templates or structure-directing agents. Typically, amines or alkylammonium salts are used in this role.[1−4] The synthetic opportunities offered by organometallic cations and coordination complexes are by comparison underdeveloped.

The use of metal complexes and organometallic species as structure-directing or templating agents is limited by their stability under the conditions needed for framework synthesis. There have been reports describing the use of metallophthalocyanines,[5−8] $Ru(bipy)_3^{2+}$,[9] Δ,Λ-$Co(en)_3^{3+}$,[10−12] Λ-$Co(en)_3^{3+}$,[13,14] $Co(tn)_3^{3+}$, *trans*-$Co(dien)_2^{3+}$,[15] $Co(NH_3)_6^{3+}$,[16] $CoCp_2^{+}$,[17−19] $Co-Cp^*_2{}^{+}$,[20,21] and a range of other chelate complexes[22] as

[†] Kennesaw State University.
[‡] Georgia Institute of Technology.
[§] Brookhaven National Laboratory.

(1) Lok, B. M.; Cannan, T. R.; Messina, C. A. *Zeolites* **1983**, *3*, 282−291.
(2) Davis, M. E.; Lobo, R. F. *Chem. Mater.* **1992**, *4*, 756−768.
(3) Gilson, J.-P. In *Zeolite Microporous Solids: Synthesis, Structure, and Reactivity*; Derouane, E. G., Lemos, F., Naccache, C., Ribeiro, F. R., Eds.; Kluwer: Dordrecht, 1992; pp 19−48.
(4) Guth, J. L.; Caullet, P.; Seive, A.; Patarin, J.; Delprato, F. In *Guidelines for Mastering the Properties of Molecular Sieves*; Barthomeuf, D., Ed.; Plenum Press: New York, 1990; pp 69−85.
(5) Balkus, K. J.; Hargis, C. D.; Kowalak, S. *ACS Symp. Ser.* **1992**, *499*, 347−354.
(6) Balkus, K. J.; Kowalak, S.; Ly, K. T.; Hargis, D. C. *Stud. Surf. Sci. Catal.* **1991**, *69*, 93−99.
(7) Balkus, K. J.; Gabrielov, A. G.; Bell, S. L.; Bedioui, F.; Roue, L.; Devynck, J. *Inorg. Chem.* **1994**, *33*, 67−72.
(8) Kowalak, S.; Balkus, K. J. *Collect. Czech. Chem. Commun.* **1992**, *57*, 774−780.
(9) Rankel, L. A.; Valyocsik, E. W. U.S. Patent 4,500,503 1985.
(10) Bruce, D. A.; Bertrand, J. A.; Occelli, M. L.; White, M. G.; Mertens, F. In *Catalysis of Organic Reactions*; Scaros, M. G., Prunier, M. L., Eds.; Marcel Dekker: New York, 1995; pp 545−551.
(11) Morgan, K.; Gainsford, G.; Milestone, N. *J. Chem. Soc., Chem. Commun.* **1995**, 425−426.
(12) Wilkinson, A. P.; Gray, M. J.; Stalder, S. M. *Mater. Res. Soc. Symp. Proc.* **1996**, *431*, 21−26.
(13) Gray, M. J.; Jasper, J.; Wilkinson, A. P.; Hanson, J. C. *Chem. Mater.* **1997**, *9*, 976−980.
(14) Stalder, S. M.; Wilkinson, A. P. *Chem. Mater.* **1997**, *9*, 2168−2173.
(15) Bruce, D. A.; Wilkinson, A. P.; White, M. G.; Bertrand, J. A. *J. Solid State Chem.* **1996**, *125*, 228−233.
(16) Morgan, K. R.; Gainsford, G. J.; Milestone, N. B. *Chem Commun.* **1997**, 61−62.
(17) Valyocsik, E. W. U.S. Patent 4,568,654, 1986.
(18) Balkus, K. J.; Shepelev, S. *Prepr. Pap. Am. Chem. Soc., Div. Petr.* **1993**, *38*, 512−515.
(19) Balkus, K. J.; Gavrielov, A. G.; Sandler, N.; Jacob, T. North American Catalysis Society, Snowbird, Utah 1995; Meeting Abstracts, T115−T116.
(20) Balkus, K. J.; Gabrielov, A. G.; Zones, S. I. *Stud. Surf. Sci. Catal.* **1995**, *97*, 519−525.
(21) Freyhardt, C. C.; Tsapatsis, M.; Lobo, R. F.; Balkus, K. J.; Davis, M. E. *Nature* **1996**, *381*, 295−298.

10.1021/cm9901921 CCC: $18.00
Published on Web 07/17/1999

additives to molecular sieve synthesis gels (en = 1,2-diaminoethane, tn = 1,3-diaminopropane, dien = diethylenetriamine, Cp = cyclopentadiene, and Cp* = pentamethylcyclopentadiene). In general, coordination complexes such as $Co(en)_3^{3+}$ have inadequate stability at high pH and temperature to be viable for the synthesis of aluminosilicates. However, species related to $CoCp_2^+$ are useful for aluminosilicate synthesis. The preparation of the first zeolite to contain 14 T atom pores[21] using decamethylcobaltacenium as a structure-directing agent is of particular significance.

Our prior work with coordination complexes as structure-directing agents[12−15] made use of chiral Co(III) chelate complexes with N-donor ligands in the synthesis of aluminophosphate (AlPO) and gallophosphate (GaPO) materials. While many complexes of this type can be envisioned, their hydrothermal stability is often inadequate for the synthesis of AlPO or GaPO frameworks. The preparation of a sample containing single crystals suitable for structure analysis is usually more demanding of the template's stability than the synthesis of a powder. For example, we have previously attempted the preparation of aluminophosphates using $Co((\pm)chxn)_3^{3+}$ as a synthesis gel additive and found that we were unable to prepare anything other than powders due to the low hydrothermal stability of this cation (chxn = *trans*-1,2-diaminocyclohexane).

Complexes containing Co(III) with N-donor ligands were selected for use in our early work because the chemistry of this compound class is very well developed, and these species generally display slow ligand exchange kinetics. The slow kinetics provide resistance to decomposition and racemization. The use of related species with superior hydrothermal stability would clearly expand the range of materials that could be made. One approach to the development of metal complexes with higher stability is the use of a metal center with considerably slower ligand exchange kinetics than Co(III). Ir(III) forms a similar family of complexes to Co(III), and it displays extremely slow ligand exchange kinetics. The rate constant for ligand exchange between $Ir(OH_2)_6^{3+}$ and water is 1.1×10^{-10} s^{-1} at room temperature (residence time of ~300 years). This is 1 order of magnitude slower than that for Rh(III) and 4 orders of magnitude less than that for Cr(III).[23] Direct comparison with Co(III) is not possible as the hexaquo species is not stable in this case. However, the ligand exchange rates for Co(III) complexes are usually intermediate between those of Cr(III) and Rh(III). The Ir(III) water exchange rate is the slowest for any homoleptic mononuclear metal center that has been examined.[23]

As Ir(III) displays significantly slower ligand exchange kinetics than Co(III), we have begun to explore the use of Ir(III) complexes as structure-directing agents for framework synthesis. This paper reports our early work in the area: the preparation and characterization of Δ,Λ-$Ir(en)_3[Al_3P_4O_{16}]\cdot xH_2O$ and $Ir(chxn)_3[Al_2P_3O_{12}]\cdot xH_2O$. The former material contains AlPO layers and the later AlPO chains. Many different layered and chain[24−32] aluminophosphate materials are known, and it has recently been proposed that such low dimensional AlPOs may play an important role in the formation of microporous three-dimensional materials.[33]

The structural characterization of zeolites and other framework materials is often a significant problem. The AlPOs reported in this paper are no exception, the growth of crystals with adequate size and quality for structure determination was challenging. In the 1980s, the development of single-crystal diffractometers at synchrotron radiation sources led to a decrease in the crystal size necessary for structure determination,[34−36] but the detectors that were typically available limited what could be done. The routine use of area detectors such as imaging plates and in particular CCD cameras has significantly improved the situation. This technology has recently led to the structural characterization of several new framework materials[13,37−50] and the examination of subtle superstructures.[51]

Experimental Section

Sample Preparation. Several sets of synthetic conditions were explored for both the iridium- and cobalt-containing

(22) Balkus, K. J.; Kowalak, S. U.S. Patent 5,167,942, 1992.
(23) Cusanelli, A.; Frey, U.; Richens, D. T.; Merbach, A. E. *J. Am. Chem. Soc.* **1996**, *118*, 5265−5271.
(24) Jones, R. H.; Thomas, J. M.; Xu, R.; Huo, Q.; Xu, Y.; Cheetham, A. K.; Bieber, D. *J. Chem. Soc., Chem. Commun.* **1990**, 1170−1172.
(25) Tieli, W.; Long, Y.; Wenqin, P. *J. Solid State Chem.* **1990**, *89*, 392−395.
(26) Riou, D.; Loiseau, T.; Ferey, G. *J. Solid State Chem.* **1992**, *99*, 414−418.
(27) Gao, Q.; Chen, J.; Li, S.; Xu, R.; Thomas, J. M.; Light, M.; Hursthouse, M. B. *J. Solid State Chem.* **1996**, *127*, 145−150.
(28) Oliver, S.; Kuperman, A.; Lough, A.; Ozin, G. A. *Chem. Mater.* **1996**, *8*, 2391−2398.
(29) Oliver, S.; Kuperman, A.; Lough, A.; Ozin, G. A. *Inorg. Chem.* **1996**, *35*, 6373−6380.
(30) Williams, I. D.; Yu, J.; Gao, J.; Xu, R. *Chem. Commun.* **1997**, 1273−1274.
(31) Chippindale, A. M.; Turner, C. *J. Solid State Chem.* **1997**, *128*, 318−322.
(32) Jasper, J. D.; Wilkinson, A. P. *Chem. Mater.* **1997**, *10*, 11664−1667.
(33) Oliver, S.; Kuperman, A.; Ozin, G. A. *Angew. Chem., Int. Ed. Engl.* **1998**, *37*, 46−62.
(34) Eisenberger, P.; Newsam, J. M.; Leonowizc, M. E.; Vaughan, D. E. W. *Nature* **1984**, *309*, 45−47.
(35) Andrews, S. J.; Papiz, M. Z.; McMeeking, R.; Blake, A. J.; Lowe, B. M.; Franklin, K. R.; Helliwell, J. R.; Harding, M. M. *Acta Crystallogr., Sect. B* **1988**, *44*, 73−77.
(36) King, H. E.; Mundi, L. A.; Strohmaier, K. G.; Haushalter, R. C. *J. Solid State Chem.* **1991**, *92*, 1−7.
(37) Ko, Y.; Tan, K.; Parise, J. B.; Darovsky, A. *Chem. Mater.* **1996**, *8*, 493−496.
(38) Tan, K.; Darovsky, A.; Parise, J. B. *J. Am. Chem. Soc.* **1995**, *117*, 7039−7040.
(39) Tan, K.; Ko, Y.; Parise, J. B.; Darovsky, A. *Chem. Mater.* **1996**, *8*, 448−453.
(40) Tan, K.; Ko, Y.; Parise, J. B.; Park, J.-H.; Darovsky, A. *Chem. Mater.* **1996**, *8*, 2510−2515.
(41) Nobel, G. W.; Wright, P. A.; Lightfoot, P. L.; Morris, R. E.; Hudson, K. J.; Kvick, A.; Graafsma, H. *Angew. Chem., Int. Ed. Engl.* **1997**, *36*, 81−82.
(42) Noble, G. W.; Wright, P. W.; Kvick, A. *J. Chem. Soc., Dalton Trans.* **1997**, 4485−4490.
(43) Vezzalini, G.; Quartieri, S.; Galli, E.; Alberti, A.; Cruciani, G.; Kvick, A. *Zeolites* **1997**, *19*, 323−325.
(44) Camblor, M. A.; Diaz-Cabanas, M.-J.; Perez-Pariente, J.; Teat, S. J.; Clegg, W.; Shannon, I. J.; Lightfoot, P.; Wright, P. A.; Morris, R. E. *Angew. Chem., Int. Ed. Engl.* **1998**, *37*, 2122−2126.
(45) Hix, G. B.; Wragg, D. S.; Wright, P. A.; Morris, R. E. *J. Chem. Soc., Dalton Trans.* **1998**, 3359−3361.
(46) Sankar, G.; Wyles, J. K.; Jones, R. H.; Thomas, J. M.; Catlow, C. R. A.; Lewis, D. W.; Clegg, W.; Coles, S. J.; Teat, S. J. *Chem. Commun.* **1998**, 117−118.
(47) Wragg, D. S.; Hix, G. B.; Morris, R. E. *J. Am. Chem. Soc.* **1998**, *120*, 6822−6823.
(48) Jensen, T. R.; Norby, P.; Hanson, J. C.; Simonsen, O.; Skou, E. M.; Stein, P. C.; Boye, H. A. *J. Mater. Chem.* **1998**, *8*, 969−975.
(49) Jensen, J. R.; Norby, P.; Hanson, J. C.; Skou, E. M.; Stein, P. C. *J. Chem. Soc., Dalton Trans.* **1998**, 527−532.
(50) Krogh Anderson, A. M.; Norby, P.; Hanson, J. C.; Vogt, T. *Inorg. Chem.* **1998**, *37*, 876−881.

materials in an attempt to prepare samples that either contained crystals large enough for structural studies or were phase pure for powder diffraction measurements. Detailed syntheses are given for the iridium-containing samples that were used in the single-crystal diffraction studies and the materials containing $Co(chxn)_3^{3+}$ that were used in the powder diffraction studies. For all of the aluminophosphate syntheses, Vista Catapal B (pseudoboehmite 81.32% Al_2O_3) was used as the aluminum source. The phosphoric acid (85%) and tetramethylammonium hydroxide (25% aqueous solution) were obtained from Fisher and Aldrich, respectively.

Preparation of Ir((±)chxn)$_3$Cl$_3$. A procedure closely related to that of Galsbøl and co-workers[52] was employed. Racemic *trans*-1,2-diaminocyclohexane (3.14 g, Aldrich) was dissolved in water, CO_2 was bubbled through the solution until a white precipitate started to appear, and $IrCl_3 \cdot 3H_2O$ (2.18 g) was then added. After 5 min, the solution was boiled until an orange brown solution containing a small amount of fine precipitate had formed. The mixture was then sealed in Teflon-lined Parr acid digestion vessel and heated to 170 °C for 360 h. The autoclave was cooled to room temperature. The product consisted of colorless crystals in a brown solution mixed with a black solid. The crystals were dissolved in water, and the mixture was filtered. The resulting filtrate was evaporated to dryness and a crude off-white powder, $Ir((\pm)chxn)_3Cl_3$ (0.88 g, ~22% yield based on iridium), was recovered. No attempt was made to separate the various isomeric forms of this complex.

Ir(chxn)$_3$[Al$_2$P$_3$O$_{12}$]·4H$_2$O Crystals. Small single crystals of $Ir(chxn)_3[Al_2P_3O_{12}] \cdot 4H_2O$ were synthesized from a gel with the approximate composition 1.0 Al_2O_3:2.0 H_3PO_4:45.0 H_2O:1.0 TMAOH:0.25 $Ir((\pm)chxn)_3Cl_3$ (TMAOH = tetramethylammonium hydroxide). An ~25-g batch of AlPO gel with the above composition was prepared from the aluminum source, phosphoric acid, water, and TMAOH solution and aged for 24 h while stirring. Ground crude $Ir((\pm)chxn)_3Cl_3$ (~0.47 g) was then added to a 3.39-g portion of the gel and the stirring continued for an additional 24 h. The white gel was transferred to a Teflon-lined Parr acid digestion vessel and placed in an oven at 130 °C for 96 h. The bomb was cooled, and the contents was recovered by slurrying in distilled water followed by filtration. A similar synthesis was also performed at 140 °C for 72 h using a gel made up from 0.23 g, 0.42 g, 0.78 g, 0.67 g and 0.30 g of aluminum source, phosphoric acid, water, TMAOH solution, and the crude metal complex, respectively.

Preparation of Ir(en)$_3$Cl$_3$. This compound was prepared using the procedure of Galsbøl[53] starting with $IrCl_3 \cdot 3H_2O$ and 1,2-diaminoethane. A 57% yield of $Ir(en)_3Cl_3$ was obtained.

Δ,Λ-*Ir(en)$_3$[Al$_3$P$_4$O$_{16}$]·xH$_2$O crystals.* Small single crystals of this material were prepared using the same method and gel composition as that for $Ir(chxn)_3[Al_2P_3O_{12}] \cdot 4H_2O$, with $Ir(en)_3Cl_3$ substituted for $Ir(chxn)_3Cl_3$. The single crystal examined by X-ray diffraction was obtained from a small-scale synthesis involving only 0.063 g of the metal complex and crystallization at 130 °C for 96 h. Similar hydrothermal syntheses were also carried out at 180 °C for up to 72 h, 200 °C for 128 h, and 230 °C for 40 h. The small-scale syntheses were performed in 23-mL Parr bombs using cylindrical Teflon inserts with a small well machined in one end to contain the reaction mixture.

Resolution of trans-1,2-Diaminocyclohexane. The tartrate salts $[(-)chxnH_2][(+)tart]$ (observed $[\alpha_0]_D^{20} = 11.6°$, literature value[54] 11.6°) and $[(+)chxnH_2][H(+)tart]_2 \cdot H_2O$ (observed $[\alpha_0]_D^{20} = 25.7°$, literature value[54] 25.8°) were prepared from racemic *trans*-1,2-diaminocyclohexane (Aldrich) using the procedure of Galsbøl and co-workers.[54] The free amines were isolated via an adaptation of Galsbøl's procedure.

Preparation of Co(chxn)$_3$Cl$_3$. Samples of this complex were prepared using both racemic and optically pure *trans*-1,2-diaminocyclohexane. The complex was prepared using an adaptation of Angelici's procedure[55] for $Co(en)_3Cl_3$ where *trans*-1,2-cyclohexanediamine was substituted for 1,2-diaminoethane and the oxidation was carried out with H_2O_2 rather than air.

Preparation of Co(chxn)$_3$[Al$_2$P$_3$O$_{12}$]·xH$_2$O Powder Samples. The sample of $Co((\pm)chxn)_3[Al_2P_3O_{12}] \cdot xH_2O$ used for the powder diffraction experiments was synthesized from a gel with composition 1.00 Al_2O_3:1.00 P_2O_5:50.0 H_2O:1.00 TMAOH:0.27 $Co((\pm)chxn)_3Cl_3$. Pseudoboehmite was combined with half the required H_2O and stirred. The phosphoric acid was added dropwise while stirring. The resulting gel was aged while stirring for ~20 h. A solution of TMAOH in the remaining water was then added dropwise. The ground $Co((\pm)chxn)_3Cl_3$ was slowly added. After 15 min of stirring, the gel was transferred to a Teflon-lined Parr acid digestion vessel and heated at 100 °C. The vessel was cooled after 112 h, and the contents was slurried in distilled water. The light brown orange product was then recovered by filtration.[56] Samples were also prepared using a similar general procedure but substituting $Co((+)chxn)_3Cl_3$ or $Co((-)chxn)_3Cl_3$ for the $Co((\pm)chxn)_3Cl_3$.

Other Measurements. Powder diffraction patterns were collected using a Scintag X1 diffractometer equipped with a Cu Kα radiation source and a Peltier cooled solid-state detector. Optical rotation measurements were made using a JASCO DIP-360 Digital Polarimeter.

Single-Crystal Diffraction Data Collection. Several small crystals from the AlPO samples prepared using $Ir((\pm)chxn)_3Cl_3$ and $Ir(en)_3Cl_3$ were examined at Beam Line X7B, NSLS, Brookhaven National Laboratory. Diffraction data were recorded using Fuji imaging plates and a BAS 2000 scanner. This beam line is equipped with a double-crystal Si(111) monochromator and a Rh-coated focusing mirror. The mirror provides a high-energy cutoff that effectively eliminates $\lambda/3$ contamination of the X-ray beam for the wavelength used in the microcrystal experiment. An X-ray wavelength of 1.1167 Å and a 0.5-mm pinhole collimator were used for data collection.

Diffraction data for the structure determination of the AlPO prepared using $Ir((\pm)chxn)_3Cl_3$ were collected on a colorless needle shaped crystal (150 × 15 × 15 μm) mounted with epoxy on a tapered glass fiber. A series of diffraction patterns were recorded by rotating the unoriented crystal in the X-ray beam. The center of the image plate was at $2\theta = 0°$ and a 5° segment of ϕ was recorded on each plate. Images were recorded over the range $\phi = 2-182°$ during an initial series of scans. A second overlap set of scans was performed using the same procedure but with ϕ ranging from 10 to 90°. An exposure time of 200 s/deg was employed for the first set of scans and 100 s/deg for the second overlapping set.

A colorless plate of the AlPO prepared using Δ,Λ-$Ir(en)_3Cl_3$ (100 × 100 × 10 μm) was also used for data collection. The center of each image plate was at $2\theta = -30°$ and a 5° segment of ϕ was recorded on each plate. Images were recorded over the range $\phi = 162-342°$ during an initial series of scans. A second overlapping set of scans was performed recording 10° segments of ϕ per plate with $2\theta = 0°$ and ϕ ranging from 164 to 354°. An exposure time of 200 s/deg was employed for the first set of scans and 100 s/deg for the overlapping set.

Single-Crystal Diffraction Data Analysis. The raw diffraction data for both crystals were indexed and integrated using DENZO.[57] The data were then scaled and merged using SCALEPACK.[57] Further analysis was performed using components of the SHELXTL package.[58] Anomalous scattering corrections and absorption coefficients were obtained using the program FPRIME.[59]

(51) Evans, J. S. O.; Hanson, J. C.; Sleight, A. W. *Acta Crystallogr.* **1998**, *B54*, 705−713.
(52) Galsbøl, F. *Acta Chem. Scand.* **1978**, *A32*, 757−761.
(53) Galsbøl, F.; Rasmussen, B. S. *Acta Chem. Scand.* **1982**, *A36*, 83−87.
(54) Galsbøl, F.; Steenbøl, P.; Sørensen, B. S. *Acta Chem. Scand.* **1972**, *26*, 3605−3611.
(55) Angelici, R. J. *Synthesis and Technique in Inorganic Chemistry*; Saunders: Philadelphia, 1969.
(56) Gray, M. J. M.Sc. Dissertation, Georgia Institute of Technology, Atlanta, GA, 1997.
(57) Otwinowski, Z. *Data Collection and Processing.* Proceedings of the CCP4 study weekend; Daresbury Laboratory: Warrington, 1993.
(58) Sheldrick, G. *SHELXTL PC* V 5.03; Siemens Analytical X-ray: Madison WI, 1990.

Table 1. Crystal Data and Details of the Structure Refinement for $Ir(chxn)_3[Al_2P_3O_{12}]\cdot 4H_2O$

empirical formula	$Ir(N_2C_6H_{14})_3\,Al_2P_3O_{12}\cdot 4H_2O$[c]
formula weight	945.71[c]
wavelength, temperature	1.1167 Å, 293(2)K
crystal system, space group	triclinic, $P\bar{1}$
unit cell[a]	$a = 9.649(5)$ Å, $\alpha = 100.02(6)°$ $b = 12.365(9)$ Å, $\beta = 101.64(5)°$ $c = 16.083(8)$ Å, $\gamma = 104.75(7)°$
volume, Z	1765(2) Å^3, 2
density (calculated)	1.779 g/cm^3 [c]
absorption coefficient	9.747 mm^{-1}
absorption correction	none
$F(000)$	952.0
crystal size, mm	0.150 × 0.015 × 0.015
S[b]	1.37×10^{16}
θ range for data collection	2.09−27.92
index ranges	$0 \le h \le 7$, $-10 \le k \le 10$, $-12 \le l \le 11$
independent reflections	1448 [$R_{merge} = 0.114$][d]
refinement method	full-matrix least-squares on F^2
data/restraints/parameters	1448/50/153
goodness of fit on F^2	1.109
final R indices [966 reflections $I > 2\sigma I$][e]	$R_F = 0.1284$, $R_{wF^2} = 0.3147$
R indices all data[e]	$R_F = 0.1759$ $R_{wF^2} = 0.3591$
largest difference peak and hole	1.586 and −1.020 e Å^3

[a] A unit cell was determined separately for each recorded image. The cell constants are mean values and the esd's were determined from an analysis of the determination's repeatability. [b] Scattering power, $S = [F_{000}/V_U]^2\, V_C\lambda^3$, V_U = volume of unit cell, V_C = crystal volume. [c] Values include hydrogen atoms that were not located in the refinement. [d] $R_{merge} = \sum|(I_o - I_m)|/\sum I_o$, obtained from SCALEPACK; m, mean. [e] $R_F = \sum||F_o| - |F_c||/\sum|F_o|$, $R_{wF^2} = \{\sum[w(F_o^2 - F_c^2)^2]/\sum[w(F_o^2)^2]\}^{1/2}$.

$Ir(chxn)_3[Al_2P_3O_{12}]\cdot 4H_2O$ Structure Solution. A total of 1448 unique reflections were available after merging in $P\bar{1}$. The Ir was located by Patterson methods using the XPREP component of the SHELXTL package. The structural model was completed by difference Fourier methods and initially refined with restraints on all the Ir−N, N−C, and C−C bond lengths. An unrestrained refinement was subsequently performed, but the poor data-to-parameter ratio led to quite large variations in chemically equivalent bond lengths. The final refinement was performed with constraints on atomic displacement parameters and restraints on bond lengths. The following constraints were used: all N atomic displacements parameters are equivalent, all P and Al atomic displacement parameters are equivalent, all framework oxygen atomic displacement parameters are the same, all the ring carbon atomic displacement parameters are equivalent. The following restraints were used: all Ir−N, 2.10(2) Å; all Al−O, 1.72(2) Å; all bridging P−O, 1.54(2) Å; all terminal P−O, 1.48(2) Å; all N−C, 1.49(2) Å; and all C−C, 1.52(2) Å. All the hydrogen positions on the metal complex were placed geometrically and refined in riding mode. With the exception of the iridium, isotropic atomic displacement parameters were used for all the atoms due to the low data-to-parameter ratio. The final residuals for the data with $I > 2\sigma$ were $R_F = 0.128$ and $R_{wF^2} = 0.315$; for all data $R_F = 0.176$. Details of the crystal structure analysis are summarized in Table 1. The atomic coordinates are given in Table 2. The atom naming scheme is illustrated in Figure 1, some selected interatomic distances are shown in Table 3, and hydrogen oxygen short contacts are listed in Table 4.

Δ,Λ-$Ir(en)_3[Al_3P_4O_{16}]\cdot xH_2O$ Structure Solution. The structure was solved by direct methods in space group *Pnna*. All the hydrogen atoms on the metal complex were placed geometrically and refined in riding mode. Anisotropic atomic displacement parameters were only used for the iridium, phosphorus and aluminum atoms due to the low data-to-parameter ratio. Only reflections in 0.9−4.0 Å range were used in the final refinement due to the low reliability of the other observations. The final residuals for reflections with $I > 2\sigma$ were $R_F = 0.128$ and $R_{wF^2} = 0.379$; for all data $R_F = 0.157$. Details of the crystal structure refinement are summarized in Table 5. The atomic coordinates are given in Table 6. The atom naming scheme is illustrated in Figure 2, some selected interatomic distances are shown in Table 7, and hydrogen oxygen short contacts are listed in Table 8.

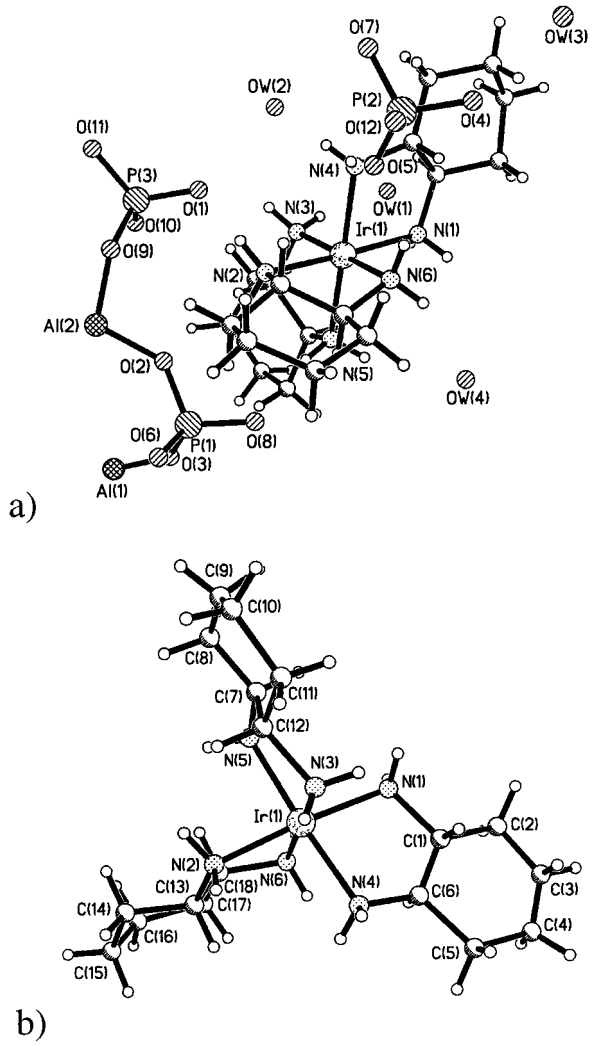

Figure 1. The $Ir(chxn)_3[Al_2P_3O_{12}]\cdot 4H_2O$ asymmetric unit showing (a) the naming scheme for the aluminophosphate chain and associated water molecules and (b) the naming scheme for the metal complex.

Results and Discussion

Aluminophosphates obtained using $Ir((\pm)\text{-}chxn)_3^{3+}$. At the start of our work using $Ir(chxn)_3^{3+}$ we anticipated the preparation of a layered AlPO belonging to the $[Al_3P_4O_{16}]^{3-}$ family of materials as our previous work using cobalt complexes and similar AlPO gel compositions/heat treatments had resulted in materials of this type. However, the X-ray diffraction structural study of the material obtained from our 130 °C synthesis revealed that the crystal examined was $Ir(chxn)_3[Al_2P_3O_{12}]\cdot xH_2O$, a compound containing AlPO chains of the type shown in Figure 3a. A comparison of the powder diffraction pattern calculated using the single-crystal structure with those measured for the bulk AlPO samples prepared at 130 and 140 °C indicated that $Ir(chxn)_3[Al_2P_3O_{12}]\cdot 4H_2O$ was the major crystalline phase in both samples. There were small amounts of an

(59) Cromer, D. T. *J. Appl. Crystallogr.* **1983**, *16*, 437.

Table 2. Atomic Coordinates ($\times 10^4$) and Isotropic Displacement Parameters ($Å^2 \times 10^3$) for $Ir(chxn)_3[Al_2P_3O_{12}]\cdot 4H_2O$

	x	*y*	*z*	U_{iso}		*x*	*y*	*z*	U_{iso}
Ir(1)	727(3)	2492(3)	2793(2)	70(2)[a]	C(17)	2925(65)	53(46)	1952(35)	70(6)
N(1)	540(40)	2694(34)	4077(14)	39(5)	C(18)	2314(59)	1071(48)	2087(28)	70(6)
N(4)	−1353(28)	1247(28)	2559(26)	39(5)	P(1)	4144(14)	4221(12)	998(10)	34(2)
C(1)	−931(48)	2000(42)	4130(32)	70(6)	P(2)	−1948(14)	−2070(12)	1809(10)	34(2)
C(2)	−911(51)	1598(51)	4969(36)	70(6)	Al(1)	4956(15)	6703(12)	703(10)	34(2)
C(3)	−2515(51)	938(44)	4853(38)	70(6)	Al(2)	1232(15)	3869(12)	−370(9)	34(2)
C(4)	−3209(66)	−185(43)	4184(32)	70(6)	P(3)	−1777(14)	3464(11)	145(10)	34(2)
C(5)	−3211(52)	203(49)	3337(37)	70(6)	O(1)	−1697(35)	2890(26)	883(18)	42(3)
C(6)	−1693(54)	978(43)	3367(27)	70(6)	O(2)	2464(22)	3929(28)	581(16)	42(3)
N(3)	−241(36)	3828(24)	2685(28)	39(5)	O(3)	4890(32)	5523(17)	1151(20)	42(3)
N(5)	2712(28)	3851(23)	3059(28)	39(5)	O(4)	−1885(34)	−2358(28)	2672(17)	42(3)
C(7)	2520(47)	5017(32)	3209(38)	70(6)	O(5)	−978(32)	−916(20)	1882(22)	42(3)
C(8)	3793(55)	6002(37)	3171(43)	70(6)	O(6)	4744(33)	3556(26)	324(15)	42(3)
C(9)	3178(55)	7012(45)	3200(40)	70(6)	O(7)	−3587(21)	−2193(22)	1403(19)	42(3)
C(10)	1697(46)	7094(43)	2744(40)	70(6)	O(8)	4390(34)	3852(27)	1827(17)	42(3)
C(11)	634(60)	5981(37)	2804(43)	70(6)	O(9)	−562(23)	3277(25)	−308(21)	42(3)
C(12)	976(43)	4838(34)	2652(39)	70(6)	O(10)	−1378(34)	4766(15)	527(20)	42(3)
N(6)	1643(41)	1110(25)	2845(26)	39(5)	O(11)	−3253(21)	3037(26)	−580(18)	42(3)
N(2)	804(44)	2192(32)	1489(14)	39(5)	O(12)	−1544(33)	−3034(22)	1251(17)	42(3)
C(13)	1233(59)	1119(40)	1277(30)	70(6)	OW1	−1077(39)	4787(31)	4632(25)	58(11)
C(14)	2035(66)	1110(44)	558(37)	70(6)	OW2	−3570(41)	2488(33)	1954(26)	69(13)
C(15)	2450(62)	6(44)	322(36)	70(6)	OW3	−3083(46)	−4398(37)	2993(29)	89(15)
C(16)	3459(62)	−114(56)	1127(31)	70(6)	OW4	4450(76)	2791(61)	4552(48)	181(27)

[a] Equivalent isotropic temperature factor. Defined as one-third of the trace of the orthogonalized U_{ij} tensor.

Table 3. Selected Bond Lengths (Å) for $Ir(chxn)_3[Al_2P_3O_{12}]\cdot 4H_2O$

Ir(1)−N(1)	2.09(2)	P(1)−O(8)	1.48(2)
Ir(1)−N(2)	2.09(2)	P(1)−O(3)	1.54(2)
Ir(1)−N(3)	2.11(2)	P(1)−O(2)	1.54(2)
Ir(1)−N(4)	2.11(3)	P(1)−O(6)	1.54(2)
Ir(1)−N(5)	2.11(2)	P(2)−O(5)	1.46(2)
Ir(1)−N(6)	2.12(2)	P(2)−O(4)	1.49(2)
N(1)−C(1)	1.49(2)	P(2)−O(7)	1.54(2)
N(4)−C(6)	1.47(2)	P(2)−O(12)	1.54(2)
N(3)−C(12)	1.50(2)	P(3)−O(1)	1.48(2)
N(5)−C(7)	1.48(2)	P(3)−O(10)	1.54(2)
N(6)−C(18)	1.49(2)	P(3)−O(9)	1.54(2)
N(2)−C(13)	1.49(2)	P(3)−O(11)	1.55(2)
C(1)−C(6)	1.50(2)	Al(1)−O(7)	1.72(2)
C(1)−C(2)	1.52(2)	Al(1)−O(3)	1.73(2)
C(2)−C(3)	1.51(2)	Al(1)−O(6)	1.72(2)
C(3)−C(4)	1.50(2)	Al(1)−O(11)	1.73(2)
C(4)−C(5)	1.52(2)	Al(2)−O(2)	1.71(2)
C(5)−C(6)	1.52(2)	Al(2)−O(10)	1.72(2)
C(7)−C(12)	1.51(2)	Al(2)−O(12)	1.73(2)
C(7)−C(8)	1.51(2)	Al(2)−O(9)	1.73(2)
C(8)−C(9)	1.51(2)		
C(9)−C(10)	1.51(2)		
C(10)−C(11)	1.52(2)		
C(11)−C(12)	1.52(2)		
C(13)−C(18)	1.52(2)		
C(14)−C(15)	1.53(2)		
C(16)−C(17)	1.52(2)		

Table 4. Short Contacts (<2.7 Å) between Hydrogen and Oxygen for $Ir(chxn)_3[Al_2P_3O_{12}]\cdot 4H_2O$

short contacts	distance, Å	atoms bonded to oxygen	atoms bonded to hydrogen
O(1)−H22A	2.04(5)	P(3)	N(2)
O(1)−H23A	2.04(5)	P(3)	N(3)
O(2)−H22B	2.26(4)	P(1), Al(2)	N(2)
O(3)−H8B	2.65(7)	P(1), Al(1)	C(8)
O(5)−H4B	2.00(5)	P(2)	N(4)
O(5)−H6B	2.20(5)	P(2)	N(6)
O(5)−H13	2.50(6)	P(2)	C(13)
O(8)−H22B	2.67(5)	P(1)	N(6)
O(8)−H25B	1.92(5)	P(1)	N(5)
O(8)−H8B	2.67(6)	P(1)	C(8)
O(11)−H16A	2.56(7)	P(3), Al(1)	C(16)
OW(1)−H1B	2.42(5)	water	N(1)
OW(1)−H23B	2.59(5)	water	N(3)
OW(1)−H1	2.69(6)	water	C(1)
OW(2)−H4A	2.16(6)	water	N(4)
OW(2)−H23A	2.44(5)	water	N(3)
OW(2)−H16B	2.66(7)	water	C(16)
OW(4)−H25A	2.46(8)	water	N(5)
OW(4)−H6A	2.58(8)	water	N(6)

unidentified impurity in the 130 °C sample and larger amounts of the same impurity in the 140 °C material. The interpretation of the powder diffraction data was hindered by preferred orientation associated with the needlelike morphology found for many of the crystallites in the samples. For both the 130 and 140 °C products, there was no visual indication of any decomposition of the metal complex during the hydrothermal synthesis.

In $Ir(chxn)_3[Al_2P_3O_{12}]\cdot 4H_2O$, the $[Al_2P_3O_{12}]^{3-}$ chains run parallel to the crystallographic *a* axis and the charge balancing metal complexes are packed between them (see Figure 4) along with the water. The water sites are apparently fully occupied, and the atomic displacement parameters for these sites suggest that there is considerable static disorder around OW4. Each AlPO chain consists of corner-sharing AlO_4 and PO_4 tetrahedra linked together to form a ribbon made of edge sharing 4-rings (see Figure 3a). There are both triply and doubly bridging PO_4 units in each ribbon. The $Ir(chxn)_3^{3+}$ interacts with the AlPO chains both electrostatically and via hydrogen bonds between the N−H groups on the complex and terminal P−O groups on the chain. Although the $Ir(chxn)_3[Al_2P_3O_{12}]\cdot 4H_2O$ crystal structure is of low precision (due to a poor data-to-parameter ratio and the generally low quality of the available data), it appears that the calculated positions for the hydrogen atoms on five of the six nitrogen atoms of the complex are within 2.20 Å of terminal P−O groups on the chain (see Table 4). Three of the four distinct terminal P−O groups are involved in these interactions. We have observed hydrogen bonding between the N−H groups on metal complexes of this type and the terminal P−O groups of metal phosphate chains, layers, and frameworks in all of the materials that we have prepared using N-donor chelate complexes as structure-directing agents.

It is interesting to note that our new chain AlPO contains only two isomeric forms of $Ir(chxn)_3^{3+}$, $\Lambda(lel_2$-

Table 5. Crystal Data and Details of the Structure Refinement for Δ,Λ-Ir(en)$_3$[Al$_3$P$_4$O$_{16}$]·*x*H$_2$O (*x* ≈ 3.45)

empirical formula	$Ir(N_2C_2H_8)_3Al_3P_4O_{16}\cdot 3.45H_2O$[c]
formula weight	895.49[c]
temperature	293(2) K
wavelength	1.1167 Å
crystal system, space group	orthorhombic, *Pnna*
unit cell[a]	*a* = 8.548(5) Å
	b = 21.983(14) Å
	c = 13.970(9) Å
volume, *Z*	2625(3) Å^3, 4
density (calculated)	2.266 g/cm^3
absorption coefficient	14.033 mm^{-1}
absorption correction	none
F(000)	1762
crystal size, mm	0.100 × 0.100 × 0.010
S[b]	6.3 × 10^{16}
θ range for data collection	2.71−40.36°
index ranges	$0 \le h \le 6, -24 \le k \le 0,$ $0 \le l \le 14$
independent reflections	1178 [$R_{merge} = 0.117$][d]
refinement method	full-matrix least-squares on F^2
data/restraints/parameters	1100/22/104[e]
goodness of fit on F^2	1.319
final *R* indices [954 reflections $I > 2\sigma I$][f]	$R_F = 0.1277$, $R_{wF}^2 = 0.3379$
R indices all data[f]	$R_F = 0.1574$, $R_{wF}^2 = 0.3864$
largest difference peak and hole	1.526 and −2.334 e Å^3

[a] A unit cell was determined separately for each recorded image. The cell constants are mean values and the esd's were obtained from an analysis of the determination's repeatability. [b] Scattering power, calculated by $S = [F_{000}/V_U]^2 V_C\lambda^3$, V_U = volume of unit cell, V_C = crystal volume. [c] Values include hydrogen atoms that were not located in the refinement. [d] $R_{merge} = \sum|(I_o - I_m)|/\sum I_o$, obtained from SCALEPACK; m, mean. [e] Only data in the 0.9−4.0 Å range (1100 of the 1178 reflections) were used in the final refinement. [f] $R_F = \sum||F_o| - |F_c||/\sum|F_o|$, $R_{wF^2} = \{\sum[w(F_o^2 - F_c^2)^2]/\sum[w(F_o^2)^2]\}^{1/2}$.

Table 6. Atomic Coordinates (×10^4) and Isotropic Displacement Parameters (Å^2 × 10^3) for Λ,Δ-Ir(en)$_3$[Al$_3$P$_4$O$_{16}$]·*x*H$_2$O (*x* ≈ 3.45)

	x	*y*	*z*	U_{iso}
Ir(1)	2500	5000	2931(2)	46(2)[a]
N(1)	1511(32)	5574(9)	3988(16)	35(7)
N(2)	1408(32)	5485(9)	1837(14)	28(6)
N(3)	607(29)	4388(11)	2998(19)	46(8)
C(1)	2493(32)	6136(12)	4056(26)	39(10)
C(2)	4174(37)	5954(15)	3907(21)	45(9)
C(3)	1658(18)	5100(17)	973(25)	64(13)
P(1)	−3561(12)	3367(3)	2867(5)	31(3)[a]
P(2)	−3538(12)	2979(3)	−967(5)	34(3)[a]
Al(1)	−753(17)	2500	2500	28(4)[a]
Al(2)	−4947(14)	2246(4)	3935(7)	40(3)[a]
O(1)	−4584(30)	3255(9)	1990(14)	51(7)
O(2)	−1874(21)	3163(7)	2617(15)	32(5)
O(3)	−4663(26)	2524(9)	−1454(14)	48(6)
O(4)	−4169(30)	2958(8)	3685(15)	46(6)
O(5)	−3554(34)	4006(8)	3156(19)	54(7)
O(6)	−3552(32)	3573(8)	−1476(17)	52(7)
O(7)	−4109(32)	3081(10)	65(12)	55(7)
O(8)	−1910(19)	2689(10)	−939(17)	48(7)
OW1	−2500	5000	4127(28)	49(10)
OW2[b]	1691(63)	5944(20)	−936(34)	85(24)
OW3	−2500	5000	1837(77)	175(38)

[a] Equivalent isotropic temperature factor. Defined as one-third of the trace of the orthogonalized U_{ij} tensor. [b] The fractional occupancy of OW2 refined to 73%. The other water sites were apparently fully occupied.

ob)-[Ir(*S*,*S*-chxn)$_2$(*R*,*R*-chxn)]$^{3+}$ (see Figure 5) and its mirror image Δ(lel$_2$ob)-[Ir(*R*,*R*-chxn)$_2$(*S*,*S*-chxn)]$^{3+}$, even though the formation of eight isomers is possible from a synthesis involving racemic *trans*-1,2-diaminocyclohexane,[53] and we did not attempt to separate the

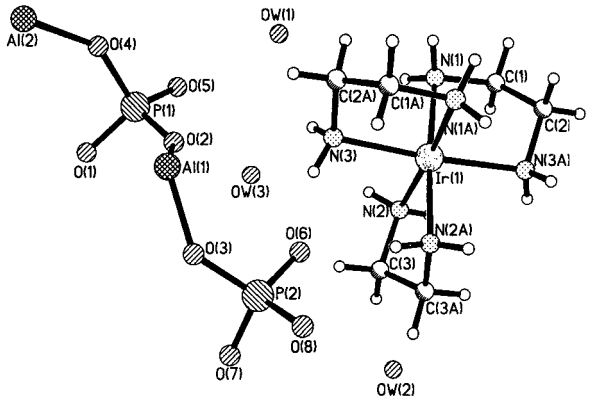

Figure 2. The asymmetric unit of Δ,Λ-Ir(en)$_3$[Al$_3$P$_4$O$_{16}$]·*x*H$_2$O.

Table 7. Selected Bond Lengths (Å) for Λ,Δ-Ir(en)$_3$[Al$_3$P$_4$O$_{16}$]·*x*H$_2$O (*x* ≈ 3.45)

2 × Ir(1)−N(1)	2.12(2)	P(2)−O(3)	1.54(2)
2 × Ir(1)−N(2)	2.09(2)	P(2)−O(6)	1.49(2)
2 × Ir(1)−N(3)	2.11(2)	P(2)−O(7)	1.54(2)
2 × N(1)−C(1)	1.50(2)	P(2)−O(8)	1.53(2)
2 × N(2)−C(3)	1.52(2)	2 x Al(1)−O(2)	1.75(2)
2 × N(3)−C(2)	1.49(2)	2 x Al(1)−O(3)	1.73(2)
C(3)−C(3)	1.51(2)	Al(2)−O(1)	1.73(2)
2 × C(1)−C(2)	1.51(2)	Al(2)−O(4)	1.74(2)
P(1)−O(5)	1.46(2)	Al(2)−O(7)	1.73(2)
P(1)−O(1)	1.52(2)	Al(2)−O(8)	1.69(2)
P(1)−O(4)	1.54(2)		
P(1)−O(2)	1.55(1)		

Table 8. Short Contacts (<2.7 Å) between Hydrogen and Oxygen for Λ,Δ-Ir(en)$_3$[Al$_3$P$_4$O$_{16}$]·4H$_2$O

short contacts	distance, Å	atoms bonded to oxygen	atoms bonded to hydrogen
O(5)−H11A	2.05(4)	P(1)	N(1)
O(5)−H12A	2.50(4)	P(1)	N(2)
O(6)−H12B	1.97(4)	P(2)	N(2)
O(6)−H13B	2.01(4)	P(2)	N(3)
2 × OW(1)−H11B	2.20(4)	water	N(1)
2 × OW(1)−H13A	2.61(4)	water	N(3)
OW(2)−H3A	2.31(7)	water	C(3)
2 × OW(3)−H13A	2.64(7)	water	N(3)

isomers. The relative stabilities of these different isomeric forms have not been studied, but data are available for the analogous cobalt(III)-containing complexes.[60] In the case of the cobalt complexes with chloride counterions, the relative abundance for equilibria involving racemic ligand is Δ,Λ-lel$_3$ > Δ,Λ lel$_2$,ob ≫ Δ,Λ-ob$_2$lel ≫ Δ,Λ-ob$_3$. This suggests that Λ(lel$_2$ob)-[Ir(*S*,*S*-chxn)$_2$(*R*,*R*-chxn)]$^{3+}$ and its mirror image are not likely to be the dominant isomers present in our AlPO syntheses if the procedure used to prepare the complex produces an equilibrium distribution of isomers. Our observation that the dominant AlPO product contains this isomer indicates that either one isomer is preferentially incorporated into the aluminophosphate or that we did not have an equilibrium distribution of isomers to start with.

In our material, only the two lel cyclohexane rings adopt well-defined chair conformations in the crystal (see Figures 1b and 5). The unusual average conformation of the ob ring may indicate the presence of some static disorder. Compounds containing Λ(lel$_3$)-[Ir(*R*,*R*-chxn)$_3$]$^{3+}$, Δ(ob$_3$)-[Ir(*R*,*R*-chxn)$_3$]$^{3+}$,[61] Λ(lel$_3$)-[Co(*R*,*R*-

(60) Harnung, S. E.; Sørensen, B. S.; Creaser, I.; Maegaard, H.; Pfenninger, U. *Inorg. Chem.* **1976**, *15*, 2123−2126.

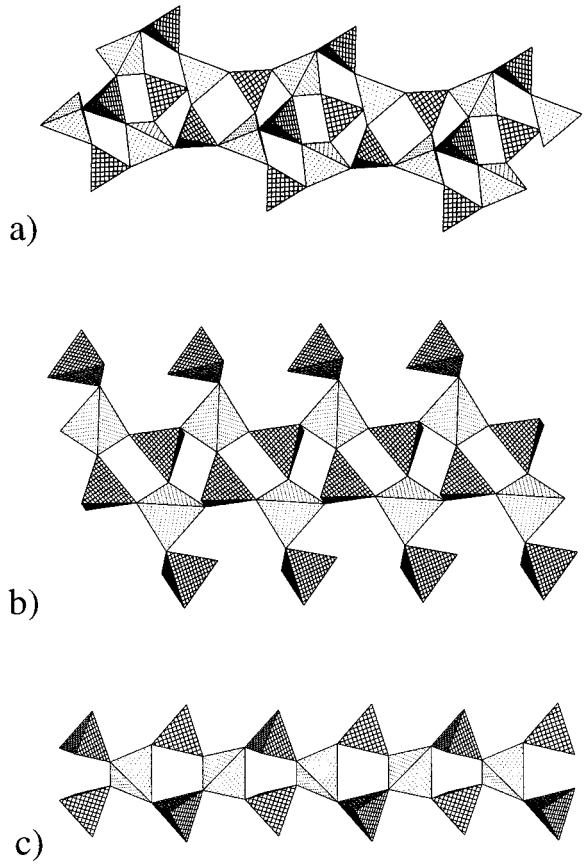

Figure 3. The $[Al_2P_3O_{12}]^{3-}$ chain found in (a) $Ir(chxn)_3[Al_2P_3O_{12}]\cdot 4H_2O$ can formally be made from (b) the $[AlP_2O_8H]^{2-}$ chains prepared by both Williams[30] and Chippindale[31] by loss of $H_2PO_4^-$. Ozin and co-workers[33] have proposed that the latter chain type can be formed from (c) parent $[AlP_2O_8H]^{2-}$ chains by a bond-breaking, chain-twisting, and bond-forming mechanism. In all the panels the PO_4 tetrahedra are crosshatched.

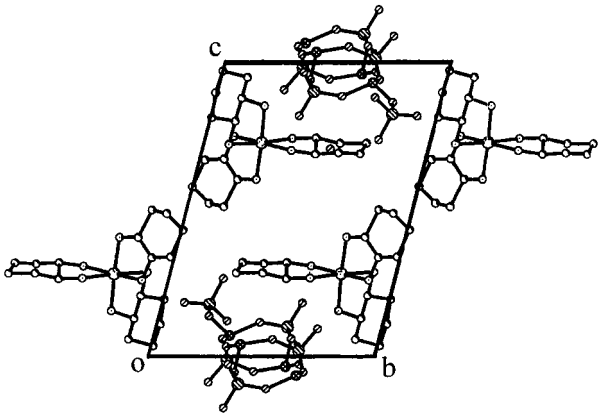

Figure 4. In $Ir(chxn)_3[Al_2P_3O_{12}]\cdot 4H_2O$ the aluminophosphate chains run parallel to the crystallographic *a* axis and the complex cations are packed between the chains. The two components of the structure interact with one another electrostatically and via hydrogen bonds.

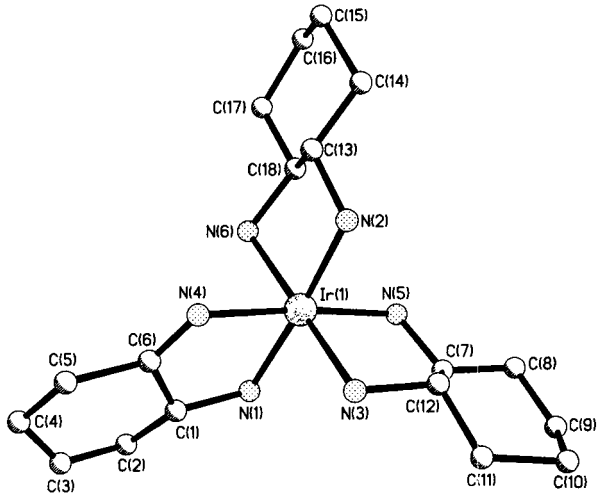

Figure 5. The $Ir(chxn)_3[Al_2P_3O_{12}]\cdot 4H_2O$ crystal examined contains only the $\Lambda(lel_2ob)$-$Ir(S,S\text{-chxn})_2(R,R\text{-chxn})]^{3+}$ isomer of the complex and its mirror image.

$chxn)_3]^{3+}$,[62] $\Lambda(lel_3)$-$[Co(S,S\text{-chxn})_3]^{3+}$,[62,63] $\Delta(lel_3)$-$[Co(R,R\text{-chxn})_3]^{3+}$,[64] $\Lambda(ob_3)$-$[Co(R,R\text{-chxn})_3]^{3+}$,[64−67] $\Lambda(lel_2ob)$-$[Co(S,S\text{-chxn})_2(R,R\text{-chxn})]^{3+}$ [68] have previously been structurally characterized. The latter species is one of the isomeric forms found in our chain AlPO material.

Chain aluminophosphates have recently received attention as possible intermediates in the formation of higher dimensional materials. Ozin and co-workers have put forward a scheme by which complex 3D, layered, and chain materials can formally be derived from a single parent $[AlP_2O_8]^{3-}$ chain (see Figure 3c).[33] While the $[Al_2P_3O_{12}]^{3-}$ chains in our new material have not previously been prepared, they fit nicely into the scheme proposed by Ozin's group. They can formally be considered to be formed by the loss of $[H_2PO_4]^-$ from $[AlP_2O_8H]^{2-}$ chains consisting of edge-sharing 4-rings with pendant singly bound PO_4 tetrahedra (see Figure 3b). A mechanism for the formation of the structure shown in Figure 3b from Ozin's parent chain (Figure 3c) was described in their review article. Interestingly, syntheses for two compounds containing chains with the connectivity shown in Figure 3b have recently been reported.[30,31] AlPO chains made up by edge-sharing 4-rings can exist in an infinite number of different isomeric forms.[33] It is interesting to note that the core of our new chain (produced by stripping away all doubly bridging phosphate) and the cores of the chains reported by both Williams[30] and Chippindale[31] (produced by stripping away all the terminal phosphate) are all trans.[33] This is illustrated in Figure 6.

Aluminophosphates Obtained Using $Co(chxn)_3^{3+}$. The single-crystal structure of $Ir(chxn)_3[Al_2P_3O_{12}]\cdot 4H_2O$ was used to calculate a powder X-ray diffraction pattern for this material's cobalt analogue. This simulation was compared with the experimental pattern for the AlPO obtained by hydrothermal synthesis using $Co((\pm)\text{-chxn})_3^{3+}$ at 100 °C. The comparison (see Figure 7)

(61) Suzuki, T.; Rude, M.; Simonsen, K. P.; Morooka, M.; Tanaka, H.; Ohba, S.; Galsbøl, F.; Fujita, J. *Bull. Chem. Soc. Jpn.* **1994**, *57*, 1013−1023.
(62) Mizuta, T.; Toshitani, K.; Miyoshi, K.; Yoneda, H. *Inorg. Chem.* **1990**, *29*, 3020−3026.
(63) Marumo, F.; Utsumi, Y.; Saito, Y. *Acta Crystallogr., Sect. B* **1970**, *26*, 1492−1498.
(64) Morooka, M.; Ohba, S.; Saito, Y. *Acta Crystallogr., Sect. B* **1991**, *47*, 910−917.
(65) Kobayashi, A.; Marumo, F.; Saito, Y. *Acta Crystallogr., Sect. B* **1972**, *28*, 2709−2715.
(66) Kobayashi, A.; Marumo, F.; Saito, Y. *Acta Crystallogr., Sect. C* **1983**, *39*, 807.
(67) Mizuta, T.; Toshitani, K.; Miyoshi, K. *Inorg. Chem.* **1991**, *30*, 572−574.
(68) Sato, S.; Saito, Y. *Acta Crystallogr., Sect. B* **1977**, *33*, 860−865.

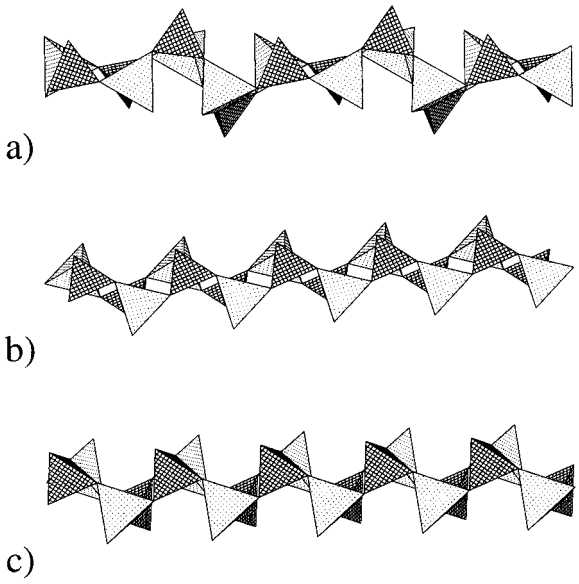

Figure 6. The core of (a) our $[Al_2P_3O_{12}]^{3-}$ chain has the same isomeric form (all trans) as the cores of the $[AlP_2O_8H]^{2-}$ chains reported by (b) Williams and (c) Chippindale. However, the conformations of the cores are slightly different. In each case all the terminal and doubly bridging phosphates have been stripped away from the chains to facilitate the comparison. In each of the drawings the PO_4 tetrahedra are crosshatched.

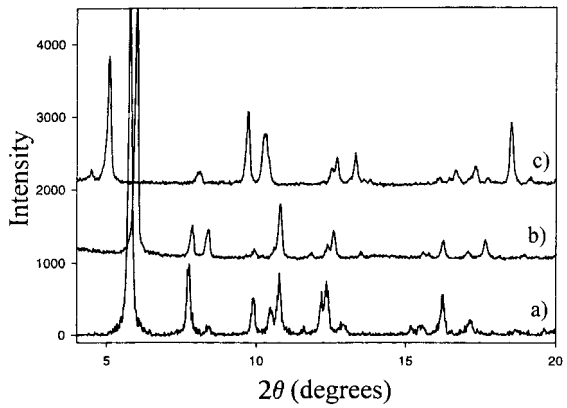

Figure 7. The calculated powder diffraction pattern for (a) a cobalt-templated aluminophosphate adopting the $Ir(chxn)_3[Al_2P_3O_{12}]\cdot 4H_2O$ structure is a reasonable match to that observed for (b) the aluminophosphate products obtained in the presence of $Co((\pm)chxn)_3^{3+}$ after taking into account small differences in lattice constants and preferred orientation. However, the pattern observed for the aluminophosphate products obtained while using (c) $Co((+)chxn)_3^{3+}$ differs markedly from pattern a. This indicates that the product produced in the presence of $Co((\pm)chxn)_3^{3+}$ is isostructural with $Ir(chxn)_3[Al_2P_3O_{12}]\cdot 4H_2O$ and different from that produced in the presence of $Co((+)chxn)_3^{3+}$.

demonstrates that the main crystalline product from the synthesis using the cobalt complex is isostructural with the iridium -containing AlPO that was prepared at higher temperature. The cobalt-containing AlPOs prepared in the presence of $Co((+)chxn)_3^{3+}$ or $Co((-)chxn)_3^{3+}$ gave powder diffraction patterns that were distinct from that obtained when using $Co((\pm)chxn)_3^{3+}$. This indicates that the different isomeric forms of $Co(chxn)_3^{3+}$ lead to different aluminophosphate products or at least a different packing of the same aluminophosphate products.

Aluminophosphates Obtained Using Δ,Λ-Ir(en)$_3^{3+}$. The X-ray structure analysis of the crystal obtained from the 130 °C AlPO preparation involving $\Delta,\Lambda\text{-}Ir(en)_3^{3+}$, indicated that the crystal was $\Delta,\Lambda\text{-}Ir(en)_3[Al_3P_4O_{16}]\cdot xH_2O$ This compound is isostructural with the previously reported layered material $\Delta,\Lambda\text{-}Co(en)_3[Al_3P_4O_{16}]\cdot xH_2O$.[11,56,69]

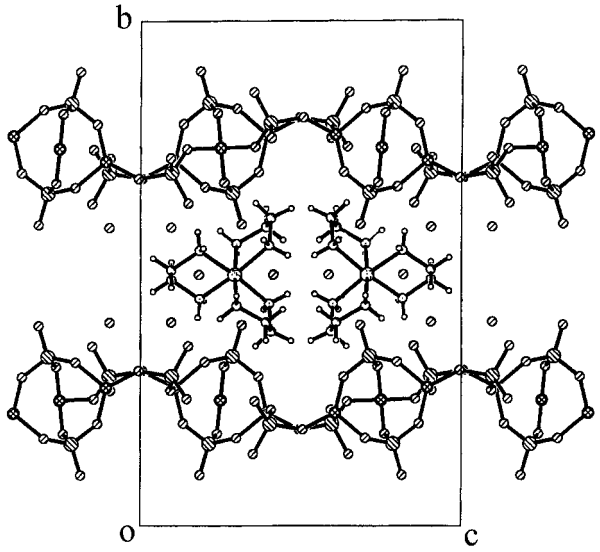

Figure 8. $\Delta,\Lambda\text{-}Ir(en)_3[Al_3P_4O_{16}]\cdot 4H_2O$ has a two-layer stacking sequence and the complexes interact with both the terminal P−O groups on the layers and the interlayer water via hydrogen bonds.

A comparison of the powder diffraction pattern calculated from the single-crystal structure with those measured for the bulk AlPO samples prepared at 130, 180, 200, and 230 °C indicated that $\Delta,\Lambda\text{-}Ir(en)_3[Al_3P_4O_{16}]\cdot xH_2O$ was the dominant crystalline phase in the samples prepared at 130 and 180 °C. The analysis of the powder diffraction data was complicated by preferred orientation. Apparently, the crystallographic *b* axis was preferentially perpendicular to the surface of the flat plate X-ray sample. This is consistent with the platelike morphology observed for many of the crystallites and the layered structure of the material (the *b* axis is perpendicular to the AlPO layers). The samples prepared at higher temperature were gray, indicating that the metal complex had at least partly decomposed during the hydrothermal syntheses. The powder diffraction patterns of the materials prepared at 200 and 230 °C were much more complicated than those of the lower temperature samples, indicating the formation of additional unidentified products. However, the strongest line present in the diffraction patterns of the low-temperature products also dominated the patterns from the high-temperature product. This may indicate the presence of $\Delta,\Lambda\text{-}Ir(en)_3[Al_3P_4O_{16}]\cdot xH_2O$ in these samples.

In $\Delta,\Lambda\text{-}Ir(en)_3[Al_3P_4O_{16}]\cdot xH_2O$, the complex cations are packed between the aluminophosphate sheets along with water lying at three crystallographically distinguishable locations (see Figure 8). The structure refinement suggests that water site OW3 is disordered and that site OW2 is not fully occupied. While several different structure types of $[Al_3P_4O_{16}]^{3-}$ layers are known, and many of them have been made using a variety of different organoamine structure-directing

(69) Bruce, D. A. Ph.D. Dissertation, Georgia Institute of Technology, Atlanta, GA, 1994.

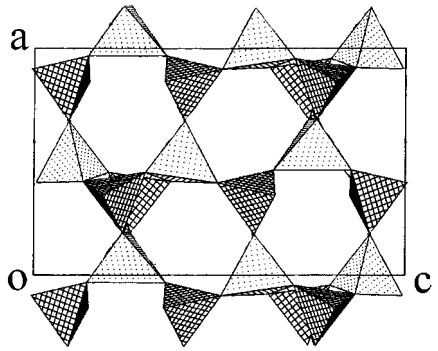

Figure 9. The layer structure found in Δ,Λ-Ir(en)$_3$[Al$_3$P$_4$O$_{16}$]·4H$_2$O has a relatively high charge density (~5.03 e/100 Å^2) and has not been observed in any of the many layered AlPOs prepared using purely organic structure-directing agents. [Al$_3$P$_4$O$_{16}$]$^{3-}$ layer structures are known with charge densities between 4.0 and 5.1 e/100 Å^2. The PO$_4$ tetrahedra in the figure are crosshatched.

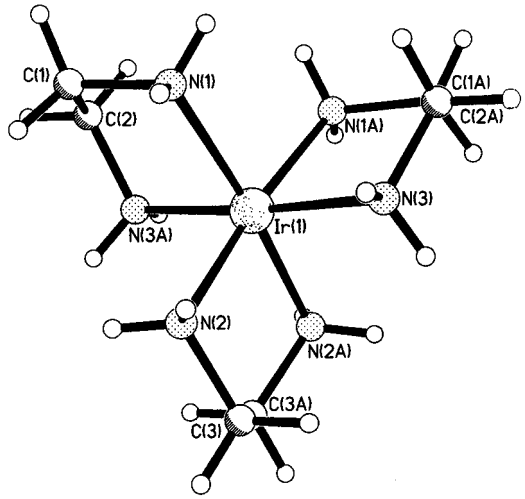

Figure 10. The metal complexes in Δ,Λ-Ir(en)$_3$[Al$_3$P$_4$O$_{16}$]·4H$_2$O adopt a lel$_3$ conformation.

agents, the variant found in this material (see Figure 9) has so far only been formed in the presence of the coordination complexes M(en)$_3^{3+}$ (M = Co, Ir). The complex cations in Δ,Λ-Ir(en)$_3$[Al$_3$P$_4$O$_{16}$]·*x*H$_2$O have an average M−N distance (2.12 Å) that is considerably longer than that found for Δ,Λ-Co(en)$_3$[Al$_3$P$_4$O$_{16}$]·*x*H$_2$O (1.98 Å). This change in cation size is seemingly accommodated by changing the interlayer spacing; the orientation of the Ir(en)$_3^{3+}$ in the interlayer space is the same as that found for Δ,Λ-Co(en)$_3$[Al$_3$P$_4$O$_{16}$]·*x*H$_2$O ($x \approx 2.8$). However, changes in interlayer spacing are also associated with the loss or gain of interlayer water, which occurs quite readily in this class of materials. The Ir(en)$_3^{3+}$ cation adopts a lel$_3$ conformation in the interlayer space of the material (see Figure 10).

In Δ,Λ-Ir(en)$_3$[Al$_3$P$_4$O$_{16}$]·*x*H$_2$O and other materials of this type, the cations interact with the AlPO layers both via hydrogen bonds and electrostatically. Even though our crystal structure of Δ,Λ-Ir(en)$_3$[Al$_3$P$_4$O$_{16}$]·*x*H$_2$O is of low precision due to the small amount of observed data and the relatively low quality of the data, it is possible to draw some conclusions regarding hydrogen bonding. All of the nitrogens on the metal complex have at least one N−H group involved in hydrogen bonding with terminal P−O groups on the layer (see Table 8 for interatomic distances). There are also some hydrogen bonds between water in the interlayer space and N−H groups on the metal complex. As might be expected, the distances found for the N−H short contacts with both the P−O groups of the sheet and the interlayer water are very similar to those found for the corresponding cobalt compound.

Conclusions

Structure-directing agents based on iridium(III) complexes provide a hydrothermally robust alternative to the corresponding cobalt compounds. The slight size difference between Co(III) and Ir(III) does not dramatically influence the nature of the AlPO products that are obtained from hydrothermal syntheses using complexes based upon the ligands 1,2-diaminoethane and *trans*-1,2-diaminocyclohexane. However, the very slow ligand exchange kinetics of the Ir(III) complexes facilitate the use of increased hydrothermal synthesis temperatures when compared to the corresponding Co(III) complexes. For the two systems that we have examined, the use of Ir(III) allows the synthesis temperatures to be increased by ~ 40 °C over the maximum that is viable for the corresponding cobalt complexes. This increase allowed us to prepare AlPO single crystals using Ir((±)chxn)$_3^{3+}$, whereas we could only obtain powders using the corresponding cobalt complexes. The use of iridium in place of cobalt increases the range of ligands that can be considered in constructing chelate complexes for use as structure-directing agents and may facilitate the preparation of different AlPO products from those found using cobalt complexes, as higher hydrothermal synthesis temperatures can be employed. However, the use of Ir(III) chelate complexes as structure-directing agents is limited by two factors: the high cost of iridium and the slow ligand exchange kinetics of these complexes. While slow ligand exchange kinetics are desirable from the perspective of the structure-directing agents hydrothermal stability, they hinder the preparation of the complexes. The chemistry of Ir(III) complexes is not as fully developed as that of Co(III) and many of the reported procedures for preparing Ir(III) complexes with N-donor ligands give very low yields.

Acknowledgment. We are grateful to the Molecular Design Institute at the Georgia Institute of Technology, supported under ONR contract N00014-95-1-1116, for partial support of this work. D.W. was a participant in the University System of Georgia Faculty Development Program at the time this work was performed. The research at Brookhaven National Laboratory was supported under contract DE-AC02-98CH10886 with the U.S. Department of Energy by its Division of Chemical Sciences, Office of Basic Energy Research.

Supporting Information Available: Tables of bond lengths and angles, anisotropic displacement parameters, hydrogen coordinates, and structure factors for Ir(chxn)$_3$-[Al$_2$P$_3$O$_{12}$]·4H$_2$O and Δ,Λ-Ir(en)$_3$[Al$_3$P$_4$O$_{16}$]·3.45H$_2$O. This material is available free of charge via the Internet at http://pubs.acs.org.

CM9901921